

Charge-Current and Neutral-Current Quasielastic Neutrino(Antineutrino) Scattering on ^{12}C with Realistic Spectral and Scaling Functions

**A.N. Antonov¹, M.V. Ivanov^{1,2}, M.B. Barbaro³, J.A. Caballero⁴,
G.D. Megias⁴, R. González-Jiménez⁵, C. Giusti⁶, A. Meucci⁶,
E. Moya de Guerra², J.M. Udías²**

¹Institute for Nuclear Research and Nuclear Energy, Bulgarian Academy of Sciences, Sofia 1784, Bulgaria

²Grupo de Física Nuclear, Departamento de Física Atómica, Molecular y Nuclear, Facultad de Ciencias Físicas, Universidad Complutense de Madrid, Madrid E-28040, Spain

³Dipartimento di Fisica, Università di Torino and INFN, Sezione di Torino, Via P. Giuria 1, 10125 Torino, Italy

⁴Departamento de Física Atómica, Molecular y Nuclear, Universidad de Sevilla, 41080 Sevilla, Spain

⁵Department of Physics and Astronomy, Ghent University, Proeftuinstraat 86, B-9000 Gent, Belgium

⁶Dipartimento di Fisica, Università degli Studi di Pavia and INFN, Sezione di Pavia, via Bassi 6 I-27100 Pavia, Italy

Abstract. Results of calculations of charge-current (CC) and neutral-current (NC) quasielastic (anti)neutrino scattering cross sections on ^{12}C target are presented. They are obtained using a realistic spectral function $S(p, \mathcal{E})$ that gives a scaling function in accordance with the (e, e') scattering data. The spectral function accounts for the nucleon-nucleon correlations by using natural orbitals from the Jastrow correlation method and has a realistic energy dependence. In the calculations the standard value of the axial mass $M_A = 1.032$ GeV is used. The role of the final-state interaction on the spectral and scaling functions, as well as on the cross sections is accounted for. Our results in the CC case are compared with those from other theoretical approaches, such as the Superscaling Approach (SuSA) and the relativistic Fermi gas (RFG), as well as with those of the relativistic mean field (RMF) and the relativistic Green's function (RGF) in the NC case. Based on the impulse approximation our calculations for the CC scattering underpredict the MiniBooNE data but agree with the data from the NOMAD experiment. The NC results are compared with the empirical data of the MiniBooNE and BNL experiments. The discussion includes the possible missing ingredients in the considered theoretical method.

1 Introduction

The phenomena of the y -scaling (*e.g.* [1–3]) and superscaling (*e.g.* [4–7]) have been observed in the inclusive electron scattering on nuclei. The theoretical concept of superscaling (a very weak dependence of the reduced cross section on the momentum transfer q at excitation energies below the quasielastic (QE) peak for large enough q and no dependence on the mass number) has been introduced within the relativistic Fermi gas (RFG) model [4–6]. It has been pointed out in [6], however, that the actual dynamical reason for the superscaling is more complex than that provided by this model. This imposes the necessity to consider the superscaling in the framework of theoretical methods that go beyond the RFG model. Later the superscaling ideas have been exploited to describe the charge-current (CC) (anti)neutrino-nuclei scattering cross sections for intermediate to high energies [8,9]. Many theoretical models, such as the RFG, the RPA, the relativistic mean-field (RMF) model, the relativistic Greens function (RGF) model, the coherent density fluctuation model (CDFM), the phenomenological SuSA approach, the spectral function models and others (see, *e.g.*, [7, 10–21]) have been devoted to analyses of the MiniBooNE [22, 23] data on quasielastic (CCQE) scattering of neutrino on nuclei. It turned out that the empirical cross sections are underestimated by most of the nuclear models. At the same time, the necessity to account for the multinucleon excitations has been proposed and a good agreement with the MiniBooNE data has been obtained in [16, 24, 25] using the standard value of the nuclear axial form factor $M_A = 1.032 \text{ GeV}/c^2$. At the same time, it should be emphasized that the CCQE data for $\nu_\mu(\bar{\nu}_\mu)+^{12}\text{C}$ cross section measurements from 3 to 100 GeV of the NOMAD collaboration [26] do not impose an anomalously large value of M_A to be used (as in some analyses of MiniBooNE data) and have been described well by various approaches based on the impulse approximation. The superscaling analyses have been carried a step further in Ref. [27] to include neutral-current (NC) (anti)neutrino scattering cross sections from ^{12}C involving proton, as well as neutron knockout in the QE regime. The CDFM scaling function was applied in [28] to analyses of NC (anti)neutrino scattering on ^{12}C (“ u -channel” inclusive process). In our work [29] NCQE (anti)neutrino scattering on ^{12}C are analyzed using a realistic spectral function $S(p, \mathcal{E})$ that gives a scaling function in accordance with the (e, e') scattering data. A number of other theoretical investigations have been devoted to NC neutrino scattering on nuclei (see the references in [29]).

The main aims of our work are the following: i) To analyze CCQE (anti)neutrino cross sections on ^{12}C measured by MiniBooNE [22, 23] and NOMAD [26] by using a spectral function with realistic energy dependence and accounting for short-range NN correlations, and ii) To analyze by the above mentioned approach the NCQE neutrino cross sections on ^{12}C measured by MiniBooNE [30] and by BNL E734 experiment [31], as well as antineutrino-nucleus scattering by MiniBooNE collaboration [32, 33].

2 Charge-Current QE (Anti)Neutrino Scattering on ^{12}C

Within the PWIA (see, *e.g.*, [34, 35] and details therein) the differential cross section for the $(e, e'N)$ process factorizes in the form

$$\left[\frac{d\sigma}{d\epsilon' d\Omega' dp_N d\Omega_N} \right]_{(e, e'N)}^{PWIA} = K \sigma^{eN}(q, \omega; p, \mathcal{E}, \phi_N) S(p, \mathcal{E}), \quad (1)$$

where σ^{eN} is the electron-nucleon cross section for a moving off-shell nucleon, K is a kinematical factor and $S(p, \mathcal{E})$ is the spectral function giving the probability to find a nucleon of certain momentum and energy in the nucleus. In Eq. (1) p is the missing momentum and \mathcal{E} is the excitation energy of the residual system. The scaling function can be represented in the form:

$$F(q, \omega) \cong \frac{[d\sigma/d\epsilon' d\Omega']_{(e, e')}}{\bar{\sigma}^{eN}(q, \omega; p = |y|, \mathcal{E} = 0)}, \quad (2)$$

where the electron-single nucleon cross section $\bar{\sigma}^{eN}$ is taken at $p = |y|$, y being the smallest possible value of p in electron-nucleus scattering for the smallest possible value of the excitation energy ($\mathcal{E} = 0$). In the PWIA the scaling function Eq. (2) is simply given by the spectral function

$$F(q, \omega) = 2\pi \iint_{\Sigma(q, \omega)} p dp d\mathcal{E} S(p, \mathcal{E}), \quad (3)$$

where $\Sigma(q, \omega)$ represents the kinematically allowed region.

In the RFG model the scaling function $f_{\text{RFG}}(\psi') = k_F \cdot F$ has the form [6]:

$$f_{\text{RFG}}(\psi') \simeq \frac{3}{4} (1 - \psi'^2) \theta(1 - \psi'^2). \quad (4)$$

In Ref. [35] more information about the spectral function was extracted within PWIA from the experimentally known scaling function. It contains effects beyond the mean-field approximation leading to a realistic energy dependence and accounts for short-range NN correlations. It is written in the form:

$$S(p, \mathcal{E}) = \sum_i 2(2j_i + 1)n_i(p)L_{\Gamma_i}(\mathcal{E} - \mathcal{E}_i), \quad (5)$$

where the Lorentzian function is used:

$$L_{\Gamma_i}(\mathcal{E} - \mathcal{E}_i) = \frac{1}{\pi} \frac{\Gamma_i/2}{(\mathcal{E} - \mathcal{E}_i)^2 + (\Gamma_i/2)^2} \quad (6)$$

with Γ_i being the width for a given s.p. hole state. In the calculations we used the values $\Gamma_{1p} = 6$ MeV and $\Gamma_{1s} = 20$ MeV, which are fixed to the experimental widths of the 1p and 1s states in ^{12}C [36]. In Eq. (5) the s.p. momentum

distributions $n_i(p)$ were taken firstly to correspond to harmonic-oscillator (HO) shell-model s.p. wave functions, and second, to natural orbitals (NOs) s.p. wave functions $\varphi_\alpha(\mathbf{r})$ defined in [37] as the complete orthonormal set of s.p. wave functions that diagonalize the one-body density matrix $\rho(\mathbf{r}, \mathbf{r}')$:

$$\rho(\mathbf{r}, \mathbf{r}') = \sum_{\alpha} N_{\alpha} \varphi_{\alpha}^*(\mathbf{r}) \varphi_{\alpha}(\mathbf{r}'), \quad (7)$$

where the eigenvalues N_{α} ($0 \leq N_{\alpha} \leq 1$, $\sum_{\alpha} N_{\alpha} = A$) are the natural occupation numbers. In [35] we used $\rho(\mathbf{r}, \mathbf{r}')$ obtained within the lowest-order approximation of the Jastrow correlation methods [38]. For accounting for the FSI we follow the approach given in Ref. [39] concerning two types of FSI effects, the Pauli blocking and the interaction of the struck nucleon with the spectator system by means of the time-independent optical potential (OP) $U = V - iW$. The latter can be accounted for [40] by the replacing in the PWIA expression for the inclusive electron-nucleus scattering cross section

$$\frac{d\sigma_t}{d\omega d|\mathbf{q}|} = 2\pi\alpha^2 \frac{|\mathbf{q}|}{E_{\mathbf{k}}^2} \int dE d^3p \frac{S_t(\mathbf{p}, E)}{E_{\mathbf{p}} E_{\mathbf{p}'}} \delta(\omega + M - E - E_{\mathbf{p}'}) L_{\mu\nu}^{\text{em}} H_{\text{em}, t}^{\mu\nu} \quad (8)$$

the energy-conserving delta-function by

$$\delta(\omega + M - E - E_{\mathbf{p}'}) \rightarrow \frac{W/\pi}{W^2 + [\omega + M - E - E_{\mathbf{p}'} - V]^2}. \quad (9)$$

In Eq. (8) the index t denotes the nucleon isospin, $L_{\mu\nu}^{\text{em}}$ and $H_{\text{em}, t}^{\mu\nu}$ are the leptonic and hadronic tensors, respectively, and $S_t(\mathbf{p}, E)$ is the proton (neutron) spectral function. The real (V) and imaginary (W) parts of the OP in (8) and (9) are obtained in Ref. [41] from the Dirac OP. The CC (anti)neutrino cross section in the target laboratory frame is given in the form (see for details [8, 10])

$$\left[\frac{d^2\sigma}{d\Omega dk'} \right]_{\chi} \equiv \sigma_0 \mathcal{F}_{\chi}^2, \quad (10)$$

where $\chi = +$ for neutrino-induced reaction (*e.g.*, $\nu_{\ell} + n \rightarrow \ell^{-} + p$, where $\ell = e, \mu, \tau$) and $\chi = -$ for antineutrino-induced reactions (*e.g.*, $\bar{\nu}_{\ell} + p \rightarrow \ell^{+} + n$). The quantity \mathcal{F}_{χ}^2 in (10) depends on the nuclear structure and is presented [8] as a generalized Rosenbluth decomposition containing leptonic factors and five nuclear response functions, namely charge-charge (CC), charge-longitudinal (CL), longitudinal-longitudinal (LL), vector-transverse (T) and axial-transverse (T') expressed by the nuclear tensor and the scaling function. Here we note that while the electron-nuclei scattering contains two electromagnetic response functions (longitudinal R_L and transverse R_T) and contains both isoscalar and isovector contributions, in the CCQE scattering the nuclear responses are purely isovector, typically transverse and have vector-vector, axial-axial and vector-axial contributions. To obtain the scaling function we use the spectral function

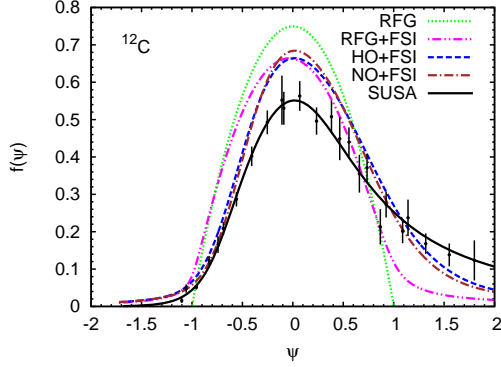


Figure 1. Results for the scaling function $f(\psi)$ for ^{12}C obtained using RFG+FSI, HO+FSI, and NO+FSI approaches are compared with the RFG and SUSA results, as well as with the longitudinal experimental data.

$S(p, \mathcal{E})$ from (5) with $n_i(p)$ corresponding to HO or NOs s.p. wave functions, and the Lorentzian function (6). We calculate the electron- ^{12}C cross section by using Eqs. (8) and (9) and the scaling function $F(q, \omega)$ within the PWIA from Eq. (3). By multiplying $F(q, \omega)$ by k_F the scaling function $f(\psi')$ is obtained. It is presented in Figure 1. As can be seen, the accounting for FSI leads to a small asymmetry in $f(\psi')$. The results of our calculations of the differential and total cross sections of CCQE $\nu(\bar{\nu})$ scattering on ^{12}C are obtained using the approaches mentioned above to evaluate the spectral and scaling functions. The results for the total cross sections obtained in [21] within the RFG+FSI, HO+FSI and NO+FSI are given in Figure 2 and compared with the SuSA results and the MiniBooNE [22, 23] and NOMAD [26] data (up to 100 GeV). All models give results that agree with the NOMAD data but underpredict the MiniBooNE ones, more seriously in the ν_μ than in $\bar{\nu}_\mu$ case. In Figure 2(b) the results for T , L and T' contributions to the cross section of NO+FSI case are presented. In Figure 2(c) the CCQE $\bar{\nu}_\mu$ - ^{12}C cross section is given. As can be seen in Figure 2(b) the maximum of the T' contribution is around the maximum of the neutrino flux at MiniBooNE experiment. The effects of the T' contribution are negligible at $E_\nu > 10$ GeV. For high $\nu_\mu(\bar{\nu}_\mu)$ energies the total cross section for ν_μ and $\bar{\nu}_\mu$ are very similar, that is consistent with the negligible contribution of T' response in this region. Only L and T channels contribute for $E_\nu > 10$ GeV explored by NOMAD experiment (where the theory is in agreement with the data). The discrepancy with the MiniBooNE data (at energies < 1 GeV) is most likely due to missing effects beyond the IA, *e.g.* those of the 2p-2h excitations that have contributions in the transverse responses. This concerns also the similar disagreement that appears when the phenomenological scaling function in SuSA is used. The latter, being extracted from the (e, e') data is a purely longitudinal QE response and thus is nearly insensitive to 2p-2h MEC contributions.

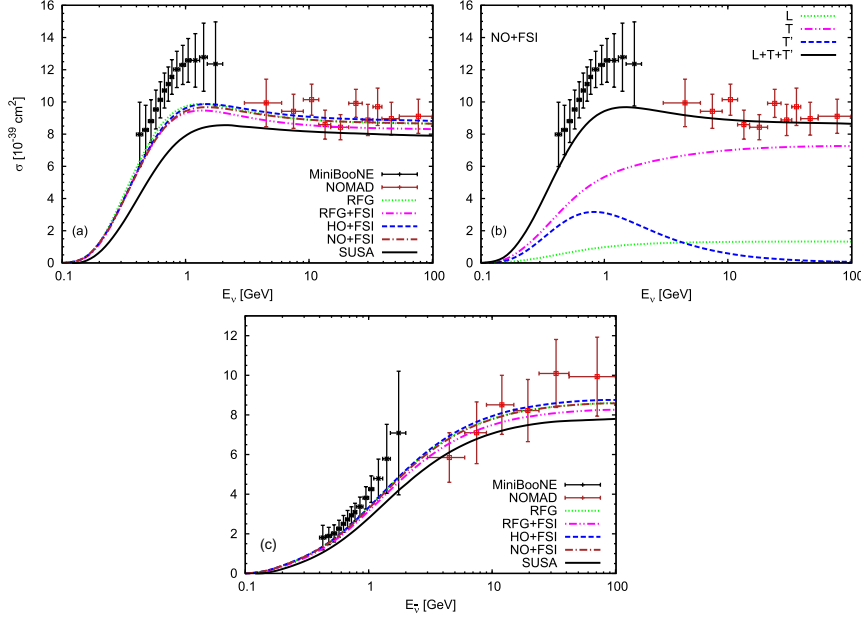


Figure 2. (a) CCQE ν_μ - ^{12}C total cross sections as a function of E_ν compared with the MiniBooNE [22] and NOMAD [26] data; $M_A = 1.032 \text{ GeV}/c^2$; (b) separated contributions (L , T , T' , $L + T + T'$) in the NO+FSI approach; (c) CCQE $\bar{\nu}_\mu$ - ^{12}C total cross section. The MiniBooNE data are from [23].

3 Neutral-Current QE Neutrino Scattering on ^{12}C

The QE electron and CCQE neutrino scattering are “ t -channel” reactions in which the outgoing lepton (with 4-momentum $K^{\mu'}$) is observed, and sum over nucleon variables is performed. In this case the Mandelstam variable $t = (K^\mu - K^{\mu'})^2$ is fixed, K^μ being the 4-momentum of the incoming lepton. In the case of NC neutrino scattering only the outgoing nucleon (with momentum P_N^μ) is observed and the outgoing neutrino is integrated over. This is a “ u -channel” process, where the Mandelstam variable $u = (K^\mu - P_N^\mu)^2$ is fixed. In this case the transfer 4-momentum $Q^\mu = (\omega, q)$ is not specified. A new transfer 4-momentum $Q'^\mu = (K^\mu - P_N^\mu) = (\omega', q')$ is introduced and new scaling variables $y^{(u)}(q', \omega')$ and $\psi^{(u)}(q', \omega')$ are defined. The cross section for the $(l, l'N)$ process within the PWIA has the form [27]:

$$\frac{d\sigma}{d\Omega_N dp_N} \simeq \bar{\sigma}_{s.n.}^{(u)} F(y', q') \quad (11)$$

with

$$F(y', q') \equiv \int_{\mathcal{D}_u} p dp \int \frac{d\mathcal{E}}{E} \Sigma \simeq F(y'), \quad (12)$$

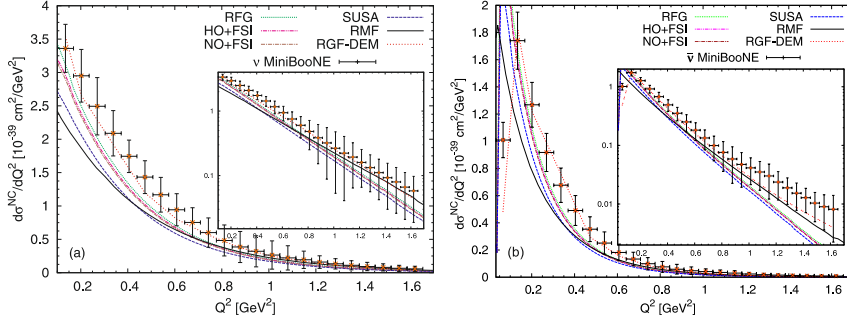


Figure 3. NCQE neutrino [(a), $\nu N \rightarrow \nu N$] and antineutrino [(b), $\bar{\nu} N \rightarrow \bar{\nu} N$] flux-averaged differential cross section computed using the RFG, HO+FSI, NO+FSI, SUSA scaling functions, RGF and RMF models and compared with the MiniBooNE data [30, 33], $M_A = 1.032 \text{ GeV}/c^2$ and strangeness $\Delta s = 0$.

where $\bar{\sigma}_{s,n}^{(u)}$ is the effective (s.n.) cross section (for details, see [27, 29]), \mathcal{D}_u being the domain of integration in the “u-channel” and Σ is the reduced cross section. Assuming that the domain \mathcal{D}_u and the “t-channel” domain \mathcal{D}_t are the same or very similar (they are different only at large \mathcal{E} and p), the results for the scaling function obtained in the (e, e') scattering can be used in the case of NC neutrino reactions. In addition to the three independent response functions L, T, T' in the “t-channel” process, in the “u-channel” inclusive scattering appear also TL, TL' and TT' response functions, though only TL response plays a significant role. The NCQE process is sensitive to both isoscalar and isovector weak currents carried by the nucleon. Using the spectral function $S(p, \mathcal{E})$ [Eq. (5)], we calculated the NCQE flux-integrated cross sections with RFG, HO+FSI, NO+FSI and SuSA scaling functions and compare them with the MiniBooNE neutrino [30] and antineutrino [33] scattering on mineral oil (CH_2) target, as well as with the results of the RMF [42, 43] and RGF [44–46] methods. The calculations are performed using the values of $M_A = 1.032 \text{ GeV}/c^2$ and of strangeness $\Delta s = 0$, where $\Delta s = F_A^s(Q^2 = 0)$, F_A^s being the strange axial isoscalar formfactor. The results are presented in Figure 3. As can be seen, the theoretical results of all models except the RGF-DEM underestimate the neutrino data in the region $0.1 < Q^2 < 0.7 \text{ GeV}^2$ ($Q^2 = 2M_N T_N$), while all theories are within the error bars for higher Q^2 . On the other hand, the same models underestimate the antineutrino data at high Q^2 . The results of our models are compared also with the BNL E734 data [31] in Figure 4. It can be seen that a good agreement exists for neutrino and antineutrino NC cross sections for $Q^2 > 0.8 \text{ GeV}^2$.

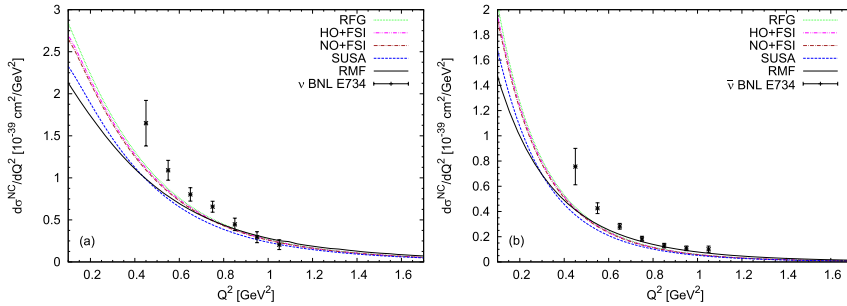


Figure 4. NCQE flux-averaged cross section: (a) $\nu p \rightarrow \nu p$ and (b) $\bar{\nu} p \rightarrow \bar{\nu} p$ compared with the BNL E734 experimental data [31]. Our results are evaluated using the RFG, HO+FSI, NO+FSI, SUSA scaling functions, and RMF model with $M_A = 1.032 \text{ GeV}/c^2$ and strangeness $\Delta s = 0$.

4 Conclusions

The results of the present work can be summarized as follows: i) The use of different spectral functions (RFG, HO, NO) gives quite similar results (*e.g.*, within 5–7% for the CCQE cross sections), signaling that the CC and NC processes are not too sensitive to the specific treatment of the bound state; ii) The FSI leads to small changes of the cross sections for different approaches in both CCQE and NCQE cases; iii) In the CCQE neutrino case all approaches based on IA underestimate the MiniBooNE data for the flux-averaged differential and total cross sections, although the shape of the cross sections is represented by NO+FSI, HO+FSI and RFG+FSI approaches. For the antineutrino the agreement is much better. All models give a good agreement with the NOMAD data; iv) In both CCQE and NCQE scattering our calculations are based on IA. They do not include *e.g.*, 2p-2h contributions induced by MEC that are very important in the $\nu(\bar{\nu})$ -nuclei scattering processes, and particular studies of their role are required.

Acknowledgements

This work was partially supported by INFN under project MANYBODY, by Spanish DGI and FEDER funds (FIS2011-28738-C02-01, FPA2013-41267), by the Junta de Andalucia, by the Spanish Consolider-Ingenio 2000 program CPAN (CSD2007-00042), by the Campus of Excellence International (CEI) of Moncloa project (Madrid) and Andalucia Tech, by the Bulgarian National Science Fund under contracts No. DFNI-T02/19 and DFNI-E02/6. R.G.J. acknowledges financial help from the Interuniversity Attraction Poles Programme initiated by the Belgian Science Policy Office.

References

- [1] G.B. West, *Phys. Rep.* **18** (1975) 263.
- [2] D.B. Day, J.S. McCarthy, T.W. Donnelly, and I. Sick, *Annu. Rev. Nucl. Part. Sci.* **40** (1990) 357.
- [3] C. Ciofi degli Atti, E. Pace, and G. Salmè, *Phys. Rev. C* **43** (1991) 1155.
- [4] W.M. Alberico, A. Molinari, T.W. Donnelly, E.L. Kronenberg, and J.W. Van Orden, *Phys. Rev. C* **38**, 1801 (1988).
- [5] M.B. Barbaro, R. Cenni, A. De Pace, T.W. Donnelly, and A. Molinari, *Nucl. Phys. A* **643**, 137 (1998).
- [6] T.W. Donnelly and I. Sick, *Phys. Rev. C* **60**, 065502 (1999).
- [7] A.N. Antonov *et al.*, *Phys. Rev. C* **69** (2004) 044321; *Phys. Rev. C* **71** (2005) 014317.
- [8] J.E. Amaro, M.B. Barbaro, J.A. Caballero, T.W. Donnelly, A. Molinari, and I. Sick, *Phys. Rev. C* **71** (2005) 015501.
- [9] J.E. Amaro, M.B. Barbaro, J.A. Caballero, T.W. Donnelly, and C. Maieron, *Phys. Rev. C* **71** (2005) 065501.
- [10] A.N. Antonov *et al.*, *Phys. Rev. C* **74** 054603 (2006).
- [11] J.T. Sobczyk, *Phys. Rev. C* **86** (2012) 015504.
- [12] A. Meucci, M.B. Barbaro, J.A. Caballero, C. Giusti, and J.M. Udías, *Phys. Rev. Lett.* **107** (2011) 172501.
- [13] M.B. Barbaro, *J. Phys.: Conf. Ser.* **336** (2011) 012024.
- [14] G. Megias, J. Amaro, M. Barbaro, J. Caballero, and T. Donnelly, *Phys. Lett. B* **725** (2013) 170.
- [15] O. Benhar, P. Coletti, and D. Meloni, *Phys. Rev. Lett.* **105** (2010) 132301.
- [16] M. Martini and M. Ericson, *Phys. Rev. C* **87** (2013) 065501.
- [17] A. Meucci, C. Giusti, and F.D. Pacati, *Phys. Rev. D* **84** (2011) 113003.
- [18] J. Nieves, I.R. Simo, and M.V. Vacas, *Phys. Lett. B* **721** (2013) 90.
- [19] O. Lalakulich, K. Gallmeister, and U. Mosel, *Phys. Rev. C* **86** (2012) 014614.
- [20] A.M. Ankowski, *Phys. Rev. C* **86** (2012) 024616.
- [21] M.V. Ivanov, A.N. Antonov, J.A. Caballero, G.D. Megias, M.B. Barbaro, E. Moya de Guerra, and J.M. Udías, *Phys. Rev. C* **89** (2014) 014607.
- [22] A.A. Aguilar-Arevalo *et al.* (MiniBooNE Collaboration), *Phys. Rev. D* **81** (2010) 092005.
- [23] A.A. Aguilar-Arevalo *et al.* (MiniBooNE Collaboration), *Phys. Rev. D* **88** (2013) 032001.
- [24] M. Martini, M. Ericson, G. Chanfray, and J. Marteau, *Phys. Rev. C* **81** (2010) 045502.
- [25] J. Nieves, I.R. Simo, and M.V. Vacas, *Phys. Lett. B* **707** (2012) 72.
- [26] V. Lyubushkin *et al.*, *Eur. Phys. J. C* **63** (2009) 355.
- [27] J.E. Amaro, M.B. Barbaro, J.A. Caballero, and T.W. Donnelly, *Phys. Rev. C* **73** 035503 (2006).
- [28] A.N. Antonov, M.V. Ivanov, M.B. Barbaro, J.A. Caballero, E. Moya de Guerra, M.K. Gaidarov, *Phys. Rev. C* **75** 064617 (2007).
- [29] M.V. Ivanov *et al.*, *Phys. Rev. C* **91** (2015) 034607.

- [30] A.A. Aguilar-Arevalo *et al.* (MiniBooNE Collaboration), *Phys. Rev. D* **82** (2010) 092005.
- [31] K. Abe *et al.*, *Phys. Rev. Lett.* **56** (1986) 1107; **56** (1986) 1883(E); L. A. Ahrens *et al.*, *Phys. Rev. D* **35** (1987) 785.
- [32] A.A. Aguilar-Arevalo *et al.* (MiniBooNE Collaboration), *Phys. Rev. D* **88** (2013) 032001.
- [33] A.A. Aguilar-Arevalo *et al.* (MiniBooNE Collaboration), *Phys. Rev. D* **91** (2015) 012004.
- [34] J.A. Caballero *et al.*, *Phys. Rev. C* **81** (2010) 055502.
- [35] A.N. Antonov *et al.*, *Phys. Rev. C* **83** (2011) 045504.
- [36] D. Dutta, Ph.D. thesis (Northwestern University, 1999).
- [37] P.-O. Löwdin, *Phys. Rev.* **97** (1955) 1474.
- [38] M.V. Stoitsov, A.N. Antonov, and S.S. Dimitrova, *Phys. Rev. C* **48** (1993) 74.
- [39] A.M. Ankowski and J.T. Sobczyk, *Phys. Rev. C* **77** (2008) 044311.
- [40] Y. Horikawa, F. Lenz, and N.C. Mukhopadhyay, *Phys. Rev. C* **22** (1980) 1680.
- [41] E.D. Cooper, S. Hama, B.C. Clark, and R.L. Mercer, *Phys. Rev. C* **47** (1993) 297.
- [42] M.C. Martinez, J.A. Caballero, T.W. Donnelly and J.M. Udías, *Phys. Rev. C* **77** (2008) 064604.
- [43] M.C. Martinez, J.A. Caballero, T.W. Donnelly and J.M. Udías, *Phys. Rev. Lett.* **100** (2008) 052502.
- [44] F. Capuzzi, C. Giusti and F.D. Pacati, *Nucl. Phys. A* **524** (1991) 681.
- [45] A. Meucci, F. Capuzzi, C. Giusti and F.D. Pacati, *Phys. Rev. C* **67** (2003) 054601.
- [46] R. Gonzalez-Jimenez, J.A. Caballero, A. Meucci, C. Giusti, M.B. Barbaro, M.I. Ivanov and J.M. Udías, *Phys. Rev. C* **88** (2013) 025502.